Critical Nuclear Charges for *N*-Electron Atoms

ALEXEI V. SERGEEV, SABRE KAIS

Department of Chemistry, Purdue University, 1393 Brown Building, West Lafayette, Indiana 47907

Received 18 March 1999; accepted 9 April 1999

ABSTRACT: One-particle model with a spherically-symmetric screened Coulomb potential is proposed to describe the motion of a loosely bound electron in a multielectron atom when the nuclear charge, which is treated as a continuous parameter, approaches its critical value. The critical nuclear charge, Z_c, is the minimum charge necessary to bind N electrons. Parameters of the model are chosen to meet known binding energies of the neutral atom and the isoelectronic negative ion. This model correctly describes the asymptotic behavior of the binding energy in the vicinity of the critical charge, gives accurate estimation of the critical charges in comparison with ab initio calculations for small atoms, and is in full agreement with the prediction of the statistical theory of large atoms. Our results rule out the stability of doubly charged atomic negative ions in the gas phase. Moreover, the critical charge obeys the proposed inequality, $N - 2 \le Z_c \le N - 1$. We show that in the presence of a strong magnetic field many atomic dianions become stable. Int J Quant Chem 75: 533–542, 1999

Key words: critical nuclear charges; *N*-electron atoms; stability of atomic dianions

Introduction

The question of stability of a given quantum system of charged particles is of fundamental importance in atomic, molecular, and nuclear physics. When the charge of one of the particles varies, the system might go from stable to metastable or to unstable configurations. Consider, for example, the ground-state energy of the two-electron atom as a function of the nuclear charge Z. Positive integer nuclear charges correspond to stable systems such as H^- ($Z = 1$), He ($Z = 2$), Li^+ ($Z = 3$), etc. However, when the charge is less than the critical charge $Z_c = 0.911$, the minimum charge necessary to bind two electrons, the ground state, ceases to exist and becomes absorbed by the continuum [1, 2].

The calculation of the critical nuclear charge, Z_c, for two-electron atoms has a long history [1, 3, 4] with controversial results of whether or not the value of Z_c is the same as the radius of convergence, Z^*, of the perturbation series in $1/Z$. Baker

Correspondence to: S. Kais.
Contract grant sponsor: NSF.
Contract grant number: CHE-9733189.
Contract grant sponsor: ONR.
Contract grant number: N00014-97-1-0192.

CCC 0020-7608 / 99 / 040533-10

et al. [2] have performed a 400-order perturbation calculation to resolve this controversy and found that Z^* is equal to Z_c, which is approximately 0.911. For N-electron atom, Lieb [5] proved that the number of electrons, N_c, that can be bound to an atom of nuclear charge, Z, satisfies $N_c < 2Z + 1$. With this rigorous mathematical result, only the instability of the dianion H^{2-} has been demonstrated [5]. For larger atoms, $Z > 1$, the corresponding bound on N_c is not sharp enough to be useful in ruling out the existence of other dianions. However, Herrick and Stillinger [24] estimated the critical charge for neon isoelectronic sequence, $Z_c \simeq 8.74$. Cole and Perdew [6] also confirmed this result for $N = 10$ by density functional calculations and ruled out the stability of O^{2-}. In a previous publication, we used Davidson's tables of energies as a function of Z to estimate the critical charges of atoms up to $N = 18$ [7]. However, Hogreve used large and diffuse basis sets and multireference configuration interaction to calculate the critical charges for all atoms up to $N = 19$ [8].

Recently, Serra and Kais [9, 10] found that one can describe stability of atomic ions and symmetry breaking of electronic structure configurations as quantum phase transitions and critical phenomena. This analogy was revealed [9] by using the large dimensional limit model of electronic structure configurations [11]. Quantum phase transitions can take place as some parameter in the Hamiltonian of the system is varied. For the Hamiltonian of N-electron atoms, this parameter is taken to be the nuclear charge. As the nuclear charge reaches a critical point, the quantum ground state changes its character from being bound to being degenerate or absorbed by a continuum. For two- and three-electron atoms, we have used the finite-size scaling method to obtain the critical nuclear charges. The finite-size scaling method was formulated in statistical mechanics to extrapolate information obtained from a finite system to the thermodynamic limit [12, 13]. In quantum mechanics, the finite size corresponds to the number of elements in a complete basis set used to expand the exact wave function of a given Hamiltonian [14, 15]. For the two-electron atoms with the configuration $1s^2$, the critical charge was found to be $Z_c \simeq 0.911$. The fact that this critical charge is below $Z = 1$ explains why H^- is a stable negative ion [16]. For the three-electron atoms the critical nuclear charge for the ground state was found to be $Z_c \simeq 2$, which explains why the He^- and H^{-2} are unstable negative ions [17].

Here we use a simple one-particle model to estimate the nuclear critical charge for any N-electron atom. This model has one free parameter which was fitted to meet the known binding energy of the neutral atom and its isoelectronic negative ion. The critical charges are found for atoms up to Rn ($N = 86$). For $N \leq 18$, our results are in good agreement with the configuration interaction computations of Hogreve [8]. In the following section we introduce the one-particle model and the methods to solve for the energies as a function of the nuclear charge. The third section gives the mapping of the multielectron atom to the one-particle model. The effect of the magnetic field on the stability of atoms is given in the fourth section. Finally, we discuss the stability of doubly charged atomic ions and ways to extend this model to molecular systems.

One-Particle Model

Superposition of the Coulomb and Yukawa potentials, known as the Hellmann potential [18], is widely used to represent interactions in atomic, molecular, and solid-state physics [19, 20]. Here, the model potential with two parameters γ and δ,

$$V(r) = -\frac{1}{r} + \frac{\gamma}{r}(1 - e^{-\delta r}) \qquad (1)$$

is used to approximate the interaction between a loosely bound electron and the atomic core in a multielectron atom.

Let us consider an N-electron atom with a nuclear charge Z. In atomic units, the potential of interaction between the loose electron and an atomic core consisting of the nucleus and the other $N - 1$ electrons tends to $-Z/r$ at small r and to $(-Z + N - 1)/r$ at large r. After the scaling transformation $r \to Zr$, the potential of interaction between two electrons is λ/r_{ij} with $\lambda = 1/Z$, and the potential of interaction between an electron and the nucleus is $-1/r_i$. In these scaled units the potential of interaction between a valence electron and a core tends to $-1/r$ at small r and tends to $(-1 + \gamma)/r$ with $\gamma = (N - 1)\lambda$ at large r. It is easy to see that the model (1) correctly reproduces such an effective potential both at small r and at large r. The transition region between $-1/r$ behavior and $(-1 + \gamma)/r$ behavior has the size of the core that is about $1/\delta$.

Eigenvalues of the potential (1) were found by two independent methods. The first method is a numerical method: solving the Sturm–Liouville eigenvalue problem by integration of the differential equation. The energies can be easily calculated for any quantum numbers n, l and any parameter γ, δ as long as the state is bound. The second method is a perturbation method in the small parameter, δ. The potential Eq. (1) is expanded in a power series of the form

$$V(r) = -\frac{1}{r} + \gamma\delta - \frac{1}{2}\gamma r\delta^2 + \frac{1}{6}\gamma r^2\delta^3 - \frac{1}{24}\gamma r^3\delta^4 + \cdots, \quad (2)$$

where the zero-order term is the Coulomb potential. The zero-order energy is given by the Rydberg formula $E_0 = \frac{1}{2}n^2$. To calculate the higher-order corrections, we used the Rayleigh–Schrödinger perturbation theory for the screened Coulomb potential. The result can be represented as a power series in δ:

$$E = -\frac{1}{2n^2} + \sum_{i=1}^{\infty} E_i\delta^i, \quad (3)$$

where the coefficients E_i are calculated [21] up to high orders $i \sim 100$.

$$E_1 = \gamma, \qquad E_2 = \left[-\tfrac{3}{4}n^2 + \tfrac{1}{4}l(l+1)\right]\gamma, \qquad E_3 = n^2\left[n^2 - \tfrac{1}{2}l(l+1) - \tfrac{1}{2}\right]\gamma, \ldots \quad (4)$$

The series in Eq. (3) can be summed by using quadratic Padé approximants that considerably accelerate the convergence and allow us to find complex energies of resonances when the perturbation parameter is sufficiently large [22]. For bound states, the results of Padé summation are the same as the one found by the numerical integration method.

Results for the ground and excited $2p$ states as a function of γ for several values of δ are shown in Figures 1 and 2, respectively. At $\gamma = 1$, the potential turns into a short-range Yukawa potential. Figures 1 and 2 demonstrate that the behavior of the function $E(\gamma)$ crucially depends on the existence of a bound state at $\gamma = 1$, i.e., whether or not $\delta < \delta_c^Y$, where δ_c^Y is the critical screening parameter for Yukawa potential [23] (it is approximately 1.1906 for the ground state and 0.2202 for $2p$ state). If $\delta < \delta_c^Y$, then the energy crosses the border of the continuum spectrum at $\gamma > 1$ with a

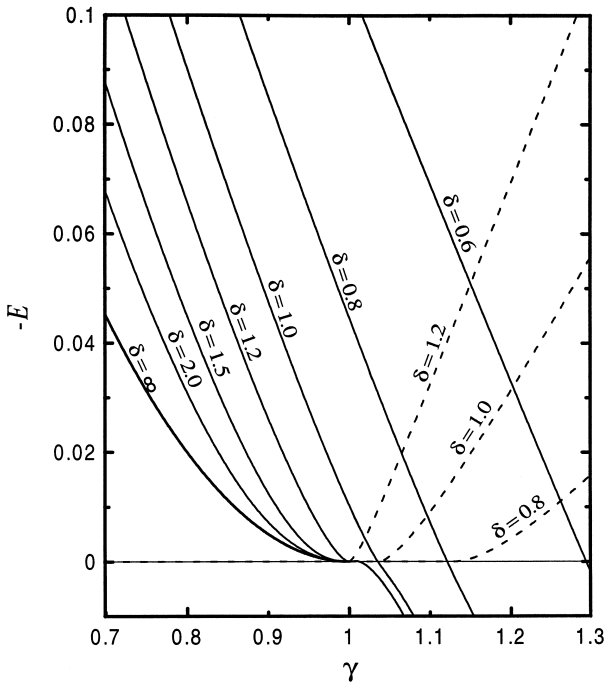

FIGURE 1. Ground-state energy, in atomic units, of the screened Coulomb potential, Eq. (1), as a function of $\gamma = (N-1)/Z$ for several values of δ. Dashed lines are the imaginary parts of the energy. The limit of $\delta \to \infty$ is also shown.

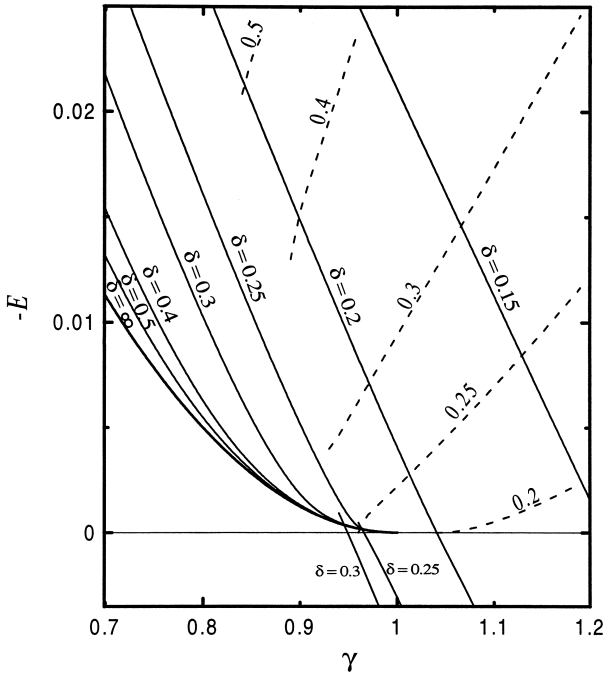

FIGURE 2. Same as in Figure 1 but for the excited $2p$ state.

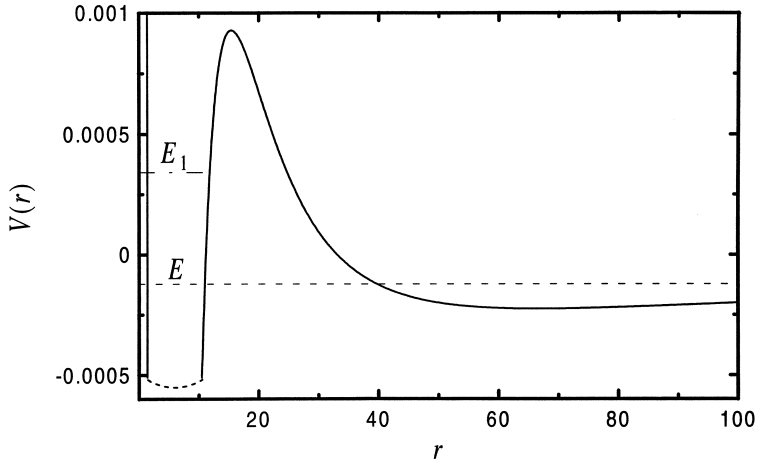

FIGURE 3. Shape of the effective potential for $l = 1$, $\delta = 0.25$, and $\gamma = 0.97$. E is energy of the bound state localized around the shallow minimum at $r \sim 60$. E_1 is the real part of energy of the quasistationary state associated with the deep minimum at relatively small r.

positive derivative, otherwise it tends to the Coulomb energy $-(1-\gamma)^2/2n^2$ and touches the border of the continuum spectrum at $\gamma \to 1$. In the latter case, the wave function becomes more and more diffuse as $\gamma \to 1$, and at the limit $\gamma = 1$ it is no longer a square-integrable wave function. We found that the results of summation of the perturbation series diverge in this region for S states ($l = 0$). However, for $l \neq 0$ states, quadratic Padé approximant converge when $\gamma \gtrsim 0.9$, but to complex values. In Figure 3, the effective potential (including the centrifugal term $-\frac{1}{2}r^2$) has a second minimum at a relatively small r that gives rise to a quasistationary state. Note that for the bound state there is another shallow minimum which is far from the origin. When $\gamma \geq 1$, the quasistationary state continues to exist while the diffuse bound state merges to the continuum spectrum.

Figure 4 shows the first derivative of the ground-state energy as a function of γ for several values of δ. It demonstrates that the first derivative at the threshold is nonzero for $\delta < \delta_c^Y$ and zero for $\delta > \delta_c^Y$.

The critical parameter $\gamma = \gamma_c$, where the energy level enters the continuum spectrum, is of a particular interest. For small δ, it can be represented in the following expansion:

$$\gamma_c(\delta) = \delta^{-1} \sum_{i=1}^{\infty} \gamma_i \delta^i. \tag{5}$$

The coefficients γ_i are found from the condition $E = 0$, where E is represented by the series (3). By

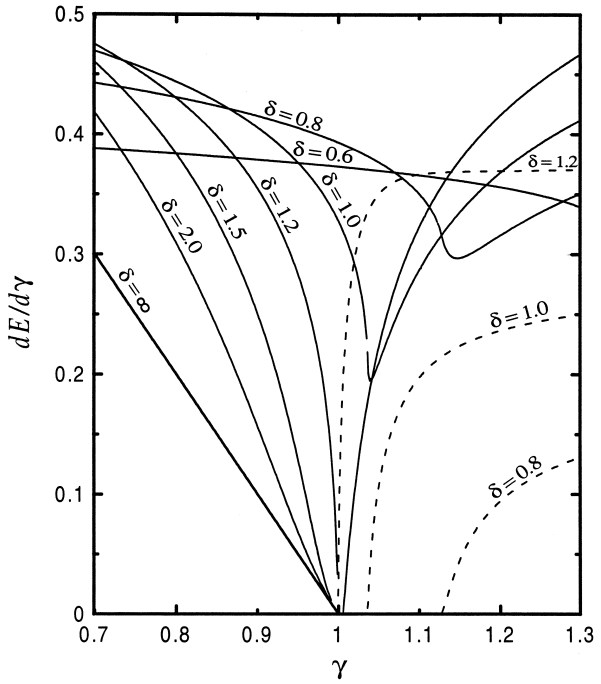

FIGURE 4. First derivative of the ground-state energy as a function of γ for the screened Coulomb potential, Eq. (1). Dashed lines are represent the imaginary parts the derivative (for quasistationary states).

elementary algebraic manipulations, we found that

$$\gamma_0 = \frac{1}{2n^2}, \qquad \gamma_1 = \frac{1}{2n^2}\left[\frac{3}{4}n^2 - \frac{1}{4}l(l+1)\right], \ldots \tag{6}$$

The series (6) is summed by quadratic Padé approximant. We found that the function $\gamma_c(\delta)$ exhibits the critical behavior at $\gamma = 1$ similar to the behavior of the energy $E(\delta)$ at $E = 0$ for Yukawa potential as shown in Figure 5. If $l = 0$, then $\gamma_c(\delta)$ approaches $\gamma = 1$ at $\delta = \delta_c^Y$ with zero derivative and a virtual state appears when $\delta > \delta_c^Y$. If $l \neq 0$, then $\gamma_c(\delta)$ crosses the line $\gamma = 1$ with nonzero derivative, and a resonance state appears when $\delta > \delta_c^Y$. The behavior of $(1 - \gamma_c)$ as a function of δ is shown in Figure 5. Note that $(1 - \gamma_c)$ is an eigenvalue of the generalized Schrödinger equation:

$$\left(-\frac{1}{2}\frac{d^2}{dr^2} + \frac{l(l+1)}{2r^2} - \frac{e^{-\delta r}}{r}\right)P(r) = (1 - \gamma_c)\frac{1 - e^{-\delta r}}{r}P(r). \quad (7)$$

Equation (7) has the same form of the Schrödinger equation for Yukawa potential,

$$\left(-\frac{1}{2}\frac{d^2}{dr^2} + \frac{l(l+1)}{2r^2} - \frac{e^{-\delta r}}{r}\right)P(r) = E^Y P(r), \quad (8)$$

with an additional weight operator $[1 - \exp(-\delta r)]/r$. Moreover, we found that the eigenvalues of Eq. (7) are similar to the eigenenergies of Yukawa potential; compare upper and lower panels of Figure 5.

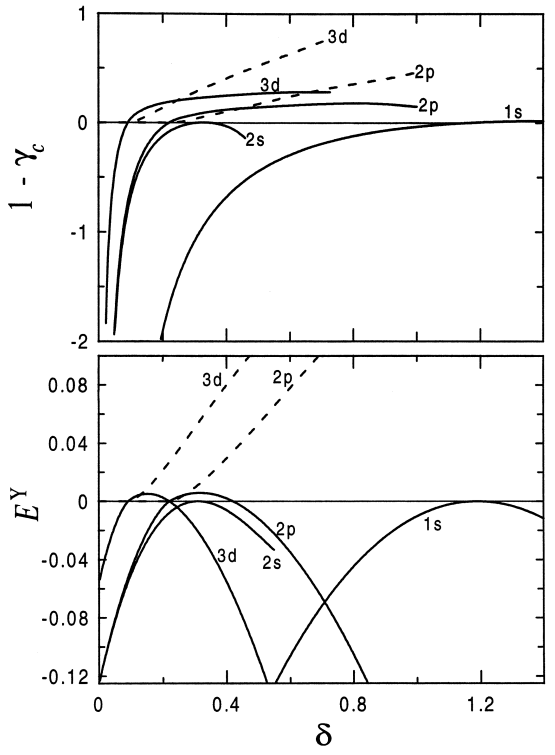

FIGURE 5. Critical parameter γ_c, Eq. (7), and the energy levels in the Yukawa potential, Eq. (8), as a function of the screening parameter δ for several states. Dashed lines represent the imaginary parts

Mapping of the *N*-Electron Atom to the One-Particle Model

Analysis of electron–electron correlations in atomic negative ions shows that one of the electrons is held much farther from the nucleus than the others [25]. It suggests a one-particle model of this electron regarded as a weakly bound electron in a short-range attractive potential. Even a simple zero-range model potential gives very good description of the photoabsorption processes in H^- [25].

The present study is not restricted to negative ions only. Our model potential (1) approximates both short-range potential of a negative ion ($Z = N - 1$) and the partially screened long-range Coulomb potential ($Z \neq N - 1$). The free parameter δ is chosen to make the binding energy $-E$ in the potential, Eq. (1), be equal to the ionization energy of an atom (or an ion) which is known from theory [26, 27] or experiments [28, 29]. Results of fitting the parameter δ for elements with $N \leq 10$ are shown in Figure 6. It is clear that δ depends on γ almost linearly. Behavior of the function $\delta(\gamma)$ near $\gamma = 1$ that corresponds to $Z = N - 1$ can be approximated by

$$\delta = \frac{\delta_0(\gamma - \gamma_1) - \delta_1(\gamma - \gamma_0)}{\gamma_0 - \gamma_1}, \quad (9)$$

where (γ_0, δ_0) are parameters corresponding to the neutral atom and (γ_1, δ_1) are parameters corresponding to the isoelectronic negative ion (if the negative ion does not exist, we use parameters corresponding to the positive ion). Ionization energy E_I is calculated by solving the Schrödinger equation with the potential (1) at $\gamma = (N - 1)\lambda$ and δ determined by Eq. (9). In essence, our method consists of extrapolation of the binding energy from two data points $\gamma = \gamma_0 = (N - 1)/N$ (neutral atom) and $\gamma = \gamma_1 = 1$ to the region of $\gamma \sim 1$.

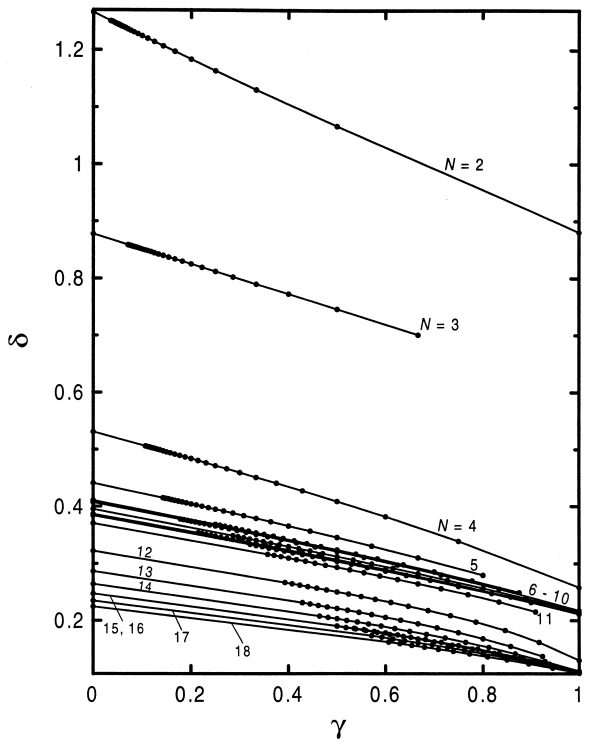

FIGURE 6. Parameter δ of the one-particle model as a function of γ for different isoelectronic series. Here N is the number of electrons.

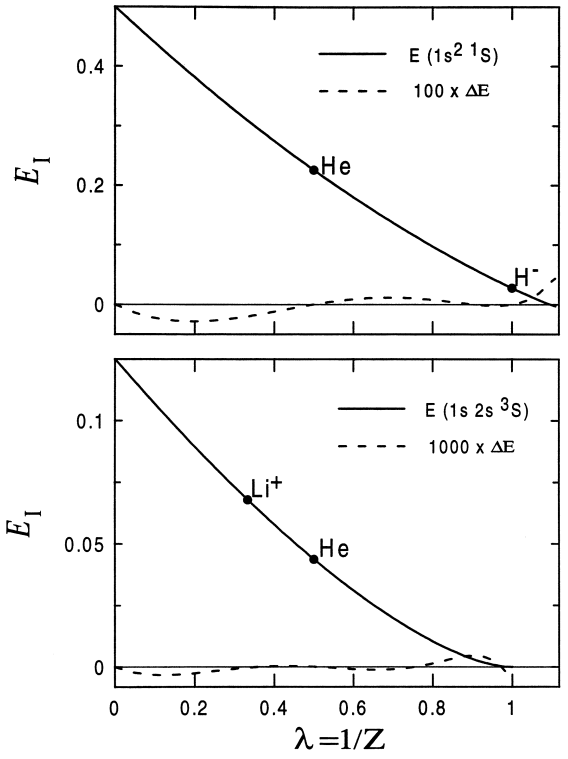

FIGURE 7. Binding energy (found by summation of the $1/Z$ expansion) for the ground state and the excited state $1s\ 2s\ ^3S$ of the two-electron isoelectronic series. Dashed curves represent the errors in our extrapolations, ΔE, relative to the exact calculations, solid line.

Let us consider the ground state and the excited state $1s\ 2s\ ^3S$ of helium isoelectronic ions. For the ground state, the dependence of the ionization energy on γ is typical for multielectron atoms having stable negative ions [8]. We reproduce the ionization energy curve, as shown in Figure 7, using only the energies of He and H^- as described above within an accuracy of 5×10^{-4}. Since $1s\ 2s\ ^3S$ state is unstable for $Z = 1$, we used ionization energies of Li^+ (instead of H^-) and He to perform the extrapolation. An accuracy of extrapolation for $1s\ 2s\ ^3S$ state is better than 10^{-5}. It is evident that direct extrapolation of the binding energy by a linear fit is inaccurate because of strong nonlinearity in the vicinity of the critical point, as shown in Figure 7. In addition, the energy has a singularity at the critical point which deteriorates further the accuracy of linear extrapolation. Our method takes advantage of the fact that an atomic core depends more weakly on λ in the vicinity of λ_c than an orbit of the outer electron that is about to dissociate. Numerical results show that the reciprocal of the core radius can be extrapolated fairly well by a linear function, Eq. (9).

The critical charges are found from the following condition:

$$E_I(\lambda_c) = 0, \qquad Z_c = 1/\lambda_c, \tag{10}$$

where E_I is the extrapolated ionization energy. Results are given in Table I. They agree (mostly within an accuracy of 0.01) with both the ab initio multireference configuration interaction calculations of Hogreve [8] and the critical charges extracted by us from Davidson's figures of isoelectronic energies [27]. In Table I, the quantum numbers of the outer-shell electron and parameters δ_0 and δ_1 are listed for neutral atoms and isoelectronic negative ions. Note that if a negative ion does not exist, then $Z_c = N - 1$ [8].

Our computations of critical charges were extended to elements with $N > 18$ with stable negative ions. Here we used experimental ionization energies from atomic data tables [29]. For many atoms with $N > 18$, the ionization energy is not a continuous function of Z because the ground-state electronic configurations of N-electron atom and

TABLE I
Critical charges for atoms with $N \leq 18$.

N (atom)	nl	δ_0	δ_1	Z_c	Z_c[a]	Z_c[b]
2 (He)	1*s*	1.066	0.881	0.912	0.91	0.92
4 (Be)	2*s*	0.339	0.258	2.864	2.85	2.86
6 (C)	2*p*	0.255	0.218	4.961	4.95	
7 (N)	2*p*	0.242	0.213	5.862	5.85	5.85
9 (F)	2*p*	0.239	0.215	7.876	7.87	7.87
10 (Ne)	2*p*	0.232	0.211	8.752	8.74	8.74
12 (Mg)	3*s*	0.162	0.130	10.880	10.86	
14 (Si)	3*p*	0.128	0.112	12.925	12.93	12.90
15 (P)	3*p*	0.123	0.110	13.796	13.78	13.79
16 (S)	3*p*	0.124	0.111	14.900	14.89	14.90
17 (Cl)	3*p*	0.120	0.109	15.758	15.74	15.75
18 (Ar)	3*p*	0.117	0.108	16.629	16.60	16.61

[a] Critical charges from ab initio, multireference configuration interaction, computations of Hogreve [8].
[b] Critical charges from Davidson's figures of isoelectronic energies [27].

$N-1$-electron positive ion may be different from that of N-electron negative ion and $N-1$-electron atom. For example, ionization of a neutral atom of scandium ($N=21$) consists of transition from the term $3d\ 4s^2\ ^2D_{3/2}$ (Sc) to $3d\ 4s\ ^3D_1$ (Sc^+), while ionization of an isoelectronic negative ion consists of transition from $4s^2\ 4p\ ^2P_{1/2}$ (Ca^-) to $4s^2\ ^1S_0$ (Ca). We assumed here that the critical charge configurations are the same as that for the negative ion. To make the ionization energy a continuous function of Z, we fixed configurations to that of the negative ion and $N-1$-electron atom (ionized state). For example, for a neutral atom of scandium ($N=21$) we considered a difference between energies of terms $4s^2\ 4p\ ^2P_{1/2}$ (Sc) and $4s^2\ ^1S_0$ (Sc^+) as a ''modified'' ionization energy which is a continuous function of the charge to be extrapolated to the region of $\gamma > 1$. Results for the critical charges are given in Table II.

Our goal here is to perform a systematic check of the stability of atomic dianions. In order to have a stable doubly negatively charged atomic ion one should require the surcharge, $S_e(N) \equiv N - Z_c(N) \geq 2$. Figure 8 shows the strong correlation between the surcharge, $S_e(N)$, and the experimental electron affinity, $EA(N-1)$. We have found that the surcharge never exceeds 2. The maximal surcharge, $S_e(86) = 1.48$, is found for the closed-shell configuration of element Rn and can be related to the peak of electron affinity of the element $N = 85$. Experimental results for negative ions of lanthanides remain unreliable [30, 31]. We did not calculate critical charges for lanthanides. Since the electron affinities of lanthanides are relatively small ≤ 0.5 eV [28], we expect that the surcharges will be small.

Dependence of the Critical Charges on a Magnetic Field

Within the one-particle model, the interaction with the magnetic field directed along the z-axis is described by the following diamagnetic term:

$$V_I(r) = \frac{B^2\rho^2}{8Z^4}; \qquad \rho^2 = x^2 + y^2, \qquad (11)$$

where the magnetic field strength B is given in atomic units (1 a.u = $2.3505\ 10^9$ G). By solving the Schrödinger equation at zero energy, with the model potential Eq. (1) plus the interaction term, Eq. (11), we found the critical parameter γ_c as a function of the scaled magnetic field $B' = B/Z_c^2$ for a given N-electron atom. By varying B', we determined the dependence of $Z_c = (N-1)/\gamma_c$ on $B = B'Z_c^2$ parametrically.

The parameter δ was set to δ_c of a free atom (at zero field). We found that the increase of the magnetic field generally leads to decrease of the critical charge. Although weakening interaction with the atomic nucleus makes the atomic core less compact and decreases the parameter δ, the increase of the diamagnetic interaction produces an opposite effect and tightens the atomic core. We assumed here, that both effects almost compensate

one another making $\delta = \text{const}$ as a good approximation.

Near the critical charge, the weak magnetic field interacts mostly with the loosely bound electron and does not change the atomic core. However, a strong magnetic field can significantly change the shape and the radius of the atomic core. This means the simple one-particle model is no longer valid.

TABLE II
Critical charges for atoms with $N > 18$.

N (atom)	nl	δ_0	δ_1	Z_c
20 Ca	4s	0.0897	0.0748	18.867
21 Sc	4p	0.0776	0.0678	19.989
22 Ti	4p	0.0764	0.0675	20.958
23 V	3d	0.0970	0.0913	21.992
24 Cr	3d	0.0966	0.0912	22.946
25 Mn	4s	0.0871	0.0751	23.863
27 Co	3d	0.0962	0.0913	25.985
28 Ni	3d	0.0959	0.0912	26.941
29 Cu	3d	0.0956	0.0911	27.900
30 Zn	4s	0.0839	0.0748	28.817
32 Ge	4p	0.0745	0.0676	30.946
33 As	4p	0.0727	0.0670	31.814
34 Se	4p	0.0728	0.0673	32.887
35 Br	4p	0.0715	0.0667	33.747
36 Kr	4p	0.0704	0.0661	34.614
38 Sr	5s	0.0573	0.0489	36.830
39 Y	5p	0.0505	0.0451	37.986
40 Zr	5p	0.0487	0.0450	38.942
41 Nb	4d	0.0614	0.0580	39.912
42 Mo	5s	0.0544	0.0485	40.802
43 Tc	5s	0.0544	0.0488	41.849
44 Ru	4d	0.0607	0.0580	42.937
45 Rh	5s	0.0537	0.0485	43.801
46 Pd	5s	0.0533	0.0485	44.797
47 Ag	5s	0.0545	0.0491	45.897
48 Cd	5s	0.0528	0.0484	46.789
50 Sn	5p	0.0486	0.0450	48.945
51 Sb	5p	0.0479	0.0447	49.807
52 Te	5p	0.0478	0.0447	50.833
53 I	5p	0.0472	0.0445	51.715
54 Xe	5p	0.0466	0.0442	52.590
57 La	6p	0.0349	0.0321	55.954
58 Ce	5d	0.0419	0.0400	56.905
60 Nd	5d	0.0423	0.0400	58.948
70 Yb	6p	0.0353	0.0322	68.985
74 W	5d	0.0415	0.0400	72.955
75 Re	5d	0.0415	0.0400	73.884
78 Pt	5d	0.0412	0.0399	76.822
79 Au	6s	0.0360	0.0338	77.656
80 Hg	6s	0.0359	0.0338	78.650
82 Pb	6p	0.0340	0.0321	80.946
83 Tl	6p	0.0341	0.0321	81.929
84 Po	6p	0.0338	0.0320	82.837
86 Rn	6p	0.0333	0.0317	84.518
89 Ac	7p	0.0256	0.0240	87.958

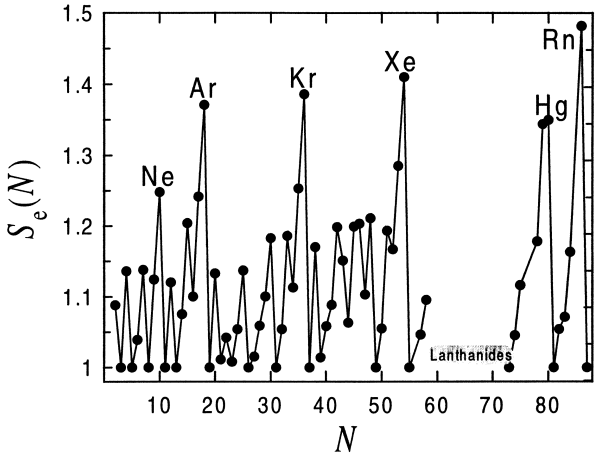

FIGURE 8. Calculated surcharge, $S_e = N - Z_c$, as a function of the number of electrons, N.

Accuracy of our model was tested for the helium isoelectronic series. Critical charges were found independently by direct variational calculations (details will be published elsewhere). Results of comparison with the one-particle model are shown in Figure 9. For weak fields, $B < 0.2$, there is a good agreement between the one-particle model and the more accurate variational calculations. For strong fields, our model significantly underestimates the critical charge because it does not take into account squeezing of the atomic core.

Results for the critical magnetic field B_c, the minimum field necessary to obtain the surcharge $S_e = 2$, for selected atoms are listed in Table III. For atoms with an external p electron, we considered both $m = 0$ and $m = \pm 1$ states. We found that $m = 0$ states are less stable in the presence of a magnetic field. However, we have found that dianions with closed-shell configurations such as O^{-2}, S^{-2}, Se^{-2}, Te^{-2}, and Po^{-2} became stable at magnetic fields of about 1–2 a.u. But dianions with an external s electron such as Ne^{-2}, Ar^{-2}, and Kr^{-2} do not exist at any magnetic field strength, B. This can be attributed to the fact that because of the different symmetry between s and p orbitals, the average $\langle \rho^2 \rangle$ for the p electron will be smaller than that for the s electron, and as a result the shift in the ionization energy will be larger in the presence of a magnetic field for an atom with a weakly bound p electron. Although it is not feasible to

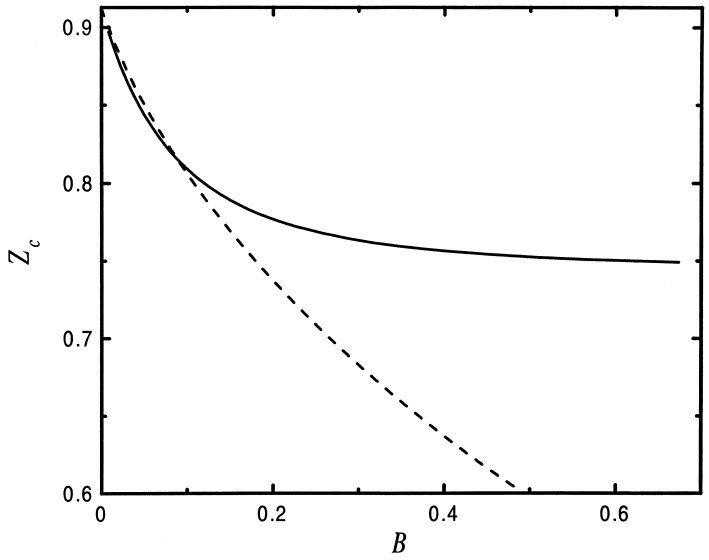

FIGURE 9. Critical charge for the helium isoelectronic series as a function of the magnetic field strength, B, in atomic units. Solid line represents the exact variational calculations and the dashed line from our one-particle model.

obtain such dianions in the laboratory, because of the strong magnetic field, they might be of considerable interest to models of magnetic white dwarf stellar atmospheres.

Conclusions

Calculation of the critical charges for N-electron atoms is of fundamental importance in atomic physics since this will determine the minimum charge to bind N electrons. Already Kato [32] and Hunziker [33] show that an atom or ion has infinitely many discrete Rydberg states if $Z > N - 1$, and the results of Zhislin and co-workers [34] show that a negative ion has only finitely many discrete states if $Z \leq N - 1$. Baker and co-workers [2] concluded, with the fact that experiment has yet to find a stable doubly negative atomic ion, the critical charge obeys the following inequality:

$$N - 2 \leq Z_c \leq N - 1. \tag{12}$$

Our numerical results confirmed this inequality and show that at most, only one electron can be added to a free atom in the gas phase. The second extra electron is not bound by singly charged negative ion because of the repulsive potential surrounding the isolated negative ion. This conclusion can be explained by examining the asymptotic form of the unscaled potential

$$V(r) = -\frac{(Z - N + 1)}{r}. \tag{13}$$

For the doubly charged negative ions, $N = Z + 2$, and this potential becomes repulsive.

Our one-particle model Hamiltonian, is simple to solve, captures the main physics of the loose electron near the critical charge, reproduces the correct asymptotic behavior of the potential, gives very accurate numerical results for the critical charges in comparison with accurate ab initio cal-

TABLE III
Critical magnetic fields, in atomic units, for *N*-electron dianions.

Dianion	N	B_c
He^{2-}	4	No
Be^{2-}	6	1.89
B^{2-}	7	1.63
N^{2-}	9	1.98
O^{2-}	10	1.70
Ne^{2-}	12	No
Mg^{2-}	14	3.36
Al^{2-}	15	1.90
Si^{2-}	16	2.65
P^{2-}	17	1.71
S^{2-}	18	1.26
Se^{2-}	36	1.32
Te^{2-}	54	1.21
Pt^{2-}	80	No
Po^{2-}	86	1.06

culations for atoms with $2 \leq N \leq 18$, and is in full agreement with the prediction of the statistical theory of Thomas–Fermi–Von Weizsacker model of large atoms. In this theory it was proved that N_c, the maximum number of electrons that can be bound to an atom of nuclear charge Z, cannot exceed Z by more than one [35].

Recently, there has been an ongoing experimental and theoretical search for doubly charged negative molecular dianions [36]. In contrast to atoms, large molecular systems can hold many extra electrons because the extra electrons can stay well separated [37]. However, such systems are challenging from both theoretical and experimental points of view. Although several authors [38–41] have studied the problem of the stability of diatomic systems as a function of the two nuclear charges, Z_1 and Z_2, there was no proof of the existence or absence of diatomic molecular dianions. Our approach might be useful in predicting the general stability of molecular dianions.

ACKNOWLEDGMENTS

We thank Dr. Pablo Serra for many useful discussions on the theory of phase transitions and stability of atomic ions. We would like to acknowledge the financial support of the NSF (grant no. CHE-9733189) and ONR (grant no. N00014-97-1-0192).

References

1. Brändas, E.; Goscinski, O. Int J Quant Chem Symp 1972, 6, 59.
2. Baker, J. D.; Freund, D. E.; Hill, R. N.; Morgan, J. D. Phys Rev A 1990, 41, 1241.
3. Stillinger, F. H. J Chem Phys 1966, 45, 3623; Stillinger, F. H.; Stillinger, D. K. Phys Rev A 1974, 10, 1109; Stillinger, F. H.; Weber, T. A. Phys Rev A 1974, 10, 1122.
4. Reinhardt, W. P. Phys Rev A 1977, 15, 802.
5. Lieb, E. H. Phys Rev Lett 1984, 52, 315; Phys Rev A 1984, 29, 3018.
6. Cole, L. A.; Perdew, J. P. Phys Rev A 1982, 25, 1265.
7. Kais, S.; Neirotti, J. P.; Serra, P. Int J Mass Spectrometry, to appear.
8. Hogreve, H. J Phys B At Mol Opt Phys 1998, 31, L439.
9. Serra, P.; Kais, S. Phys Rev Lett 1996, 77, 466.
10. Serra, P.; Kais, S. Phys Rev A 1997, 55, 238.
11. Herschbach, D. R.; Avery, J.; Goscinski, O. Dimensional Scaling in Chemical Physics; Kluwer: Dordercht, 1993; Herschbach, D. R. Int J Quant Chem 1996, 57, 295, and references therein.
12. Fisher, M. E. In Critical Phenomena, Proceedings of the 51st Enrico Fermi Summer School, Varenna, Italy, Green, M. S., Ed.; Academic: New York, 1971.
13. Privman, V., Ed. Finite Size Scaling and Numerical Simulations of Statistical Systems; World Scientific: Singapore, 1990.
14. Neirotti, J. P.; Serra, P.; Kais, S. J Chem Phys 1998, 108, 2765.
15. Serra, P.; Neirotti, J. P.; Kais, S. Phys Rev A 1998, 57, R1481.
16. Neirotti, J. P.; Serra, P.; Kais, S. Phys Rev Lett 1997, 79, 3142.
17. Serra, P.; Neirotti, J. P.; Kais, S. Phys Rev Lett 1998, 80, 5293.
18. Hellmann, B. J Chem Phys 1935, 3, 61.
19. Adamowsky, J. Phys Rev A 1985, 32, 43.
20. Bag, M.; Dutt, R.; Varshni, Y. P. J Phys B At Mol Phys 1987, 20, 5267.
21. Sergeev, A. V.; Sherstyuk, A. I. Sov Phys JETP 1982, 55, 625.
22. Sergeev, A. V.; Sherstyuk, A. I. Sov J Nucl Phys 1984, 39, 731.
23. Diaz, C. G.; Fernandez, F. M.; Castro, E. A. J Phys A Math Gen 1991, 24, 2061.
24. Herrick, D. R.; Stillinger, F. H. J Chem Phys 1975, 62, 4360.
25. Rau, A. R. P. J Astrophys Astr 1996, 17, 113.
26. Chakravorty, S. J; Gwaltney, S. R.; Davidson, E. R. Phys Rev A 1993, 47, 3649.
27. Chakravorty, S. J.; Davidson, E. R. J Phys Chem 1996, 100, 6167.
28. Hotop, H.; Lineberger, W. C. J Phys Chem Ref Data 1985, 14, 731; Berkovits, D.; Boaretto, E.; Ghelberg, S.; Heber, O.; Paul, M. Phys Rev Lett 1995, 75, 414.
29. Sugar, J.; Corliss, C. J Phys Chem Ref Data 1985, 14, Suppl. 2; Moore, C. E. Nat Stand Ref Dat Ser Nat Bur Stand (US) 1971, 1–3, 35.
30. Bates, D. R. Adv At Molec Opt Phys 1991, 27, 1.
31. Nadeau, M.-J.; Garwan, M. A.; Zhao, X.-L.; Litherland, A. E. Nucl Instr Meth Phys Res B 1997, 123, 521.
32. Kato, T. Trans Am Math Soc 1951, 70, 212.
33. Hunziker, W. Helv Phys Acta 1975, 48, 145.
34. Zhislin, G. M. Theor Math Phys 1971, 7, 571.
35. Benguria, R.; Lieb, E. H. J Phys B 1985, 18, 1045.
36. Scheller, M. K.; Compton, R. N.; Cederbaum, L. S. Science 1995, 270, 1160.
37. Wang, X. B.; Ding, C. F.; Wang, L. S. Phys Rev Lett 1998, 81, 3351.
38. Ackermann, J.; Hogreve, H. J Phys B 1992, 25, 4069.
39. Laurenzi, B. J.; Mall, M. F. Int J Quant Chem 1986, 30, 51.
40. Rebane, T. K. Sov Phys JETP 1990, 71, 1055.
41. Chen, Z.; Spruch, L. Phys Rev A 1990, 42, 133.